

1 **Soil organic matter affects arsenic and antimony sorption in anaerobic soils**

2 M. Verbeeck^a, Y. Thiry^b & E. Smolders^a

3 ^a*KU Leuven, Department of Earth and Environmental Sciences, Kasteelpark Arenberg 20 bus*
4 *2459, 3001 Leuven, Belgium and* ^b*Andra, Research and Development Division, 1-7 rue Jean-*
5 *Monnet, 92298 Châtenay-Malabry, France*

6

7 Correspondence: M. Verbeeck.

8 E-mail: mieke.verbeeck@kuleuven.be

9 **This article has been accepted for publication and undergone full peer review but has not**
10 **been through the copyediting, typesetting, pagination and proofreading process which**
11 **may lead to differences between this version and the published version.** Please cite this
12 article as <https://doi.org/10.1016/j.envpol.2019.113566>
13 ©2019. This manuscript version is made available under the CC-BY-NC-ND 4.0 license
14 <http://creativecommons.org/licenses/by-nc-nd/4.0/>

15 **Abstract**

16 Soil organic matter (SOM) affects arsenic (As) and antimony (Sb) mobility in soil under
17 waterlogged conditions by acting as an electron donor, by catalyzing redox–cycling through
18 electron shuttling and by acting as a competing ligand. This study was set up to disentangle
19 these different effects of SOM towards As and Sb sorption in anaerobic soils. Nine samples
20 were taken at different depths in an agricultural soil profile to collect samples with a natural
21 SOM gradient ($<1 - 40 \text{ g soil organic carbon kg}^{-1}$). The samples were incubated either or not
22 under waterlogged conditions in an anaerobic chamber for 63 – 70 days, and glucose (5 g C
23 kg^{-1}) was either or not added to the anaerobic incubated samples as an electron donor that
24 neither acts as an electron shuttle nor as a competing ligand. The solid-liquid distribution
25 coefficients (K_D) were measured at trace levels. The K_D values of As decreased ~ 2 orders of
26 magnitude upon waterlogging the SOM rich topsoil, while no additional changes were
27 observed when glucose was added. In contrast, smaller changes in the As K_D values were found
28 in the low SOM containing subsoil samples, unless glucose was added that mobilized As. The
29 Sb K_D values increased upon reducing conditions up to factor 20, but again only in the high
30 SOM topsoil samples. Surprisingly, the Sb immobilization during waterlogging only occurred
31 in Sb amended soils whereas the geogenic Sb was mobilized upon reducing conditions,
32 although total dissolved Sb concentrations remained low ($<10 \text{ nM}$). The change in As and Sb
33 sorption upon waterlogging was similar in the SOM rich topsoil as in the low SOM subsoil
34 amended with glucose. This suggests that the SOM dependent changes in As and Sb mobility
35 in response to soil waterlogging are primarily determined to the role of SOM as electron donor.

36 **Capsule:** The change in arsenic and antimony mobility under waterlogged conditions is largely
37 determined by the electron donor capacity of organic matter.

38

39 1. Introduction

40 Arsenic (As) and antimony (Sb) have potential hazardous effect on human health and
41 environment (Filella et al., 2009; Mandal and Suzuki, 2002). The risk of both elements to the
42 environment is determined by their toxicity and mobility in soil, and the redox potential (E_h)
43 exerts a strong influence on this mobility. First, the chemical speciation of both As and Sb is
44 pH and E_h dependent, i.e., at environmental relevant pH (4 – 9), arsenic dominates as the
45 oxyanions $H_2AsO_4^-$ and $HAsO_4^{2-}$ in oxidized systems (As(V)), while in more reduced systems,
46 the neutral species $H_3AsO_3^0$ prevails (As(III)) (Masscheleyn et al., 1991; Wilson et al., 2010).
47 The main Sb solution species at environmental relevant pH in oxidizing conditions is the
48 $Sb(OH)_6^-$ anion (Sb(V)), while in reducing conditions the neutral $Sb(OH)_3^0$ dominates (Sb(III))
49 (Filella and May, 2003; Mitsunobu et al., 2010). Second, the mobility of each chemical species
50 will be determined by its specific sorption characteristics to the reactive soil minerals or by the
51 specific solubility products of possible precipitates. For example, all As and Sb species are
52 strongly retained on iron (Fe) hydroxides by sorption reactions, however, the more oxidized
53 species are in general more strongly retained at acidic pH, while the sorption of the more
54 reduced species are more strongly retained at higher pH (Dixit and Hering, 2003; Leuz et al.,
55 2006). In addition, at elevated concentrations of As and Sb in soils (i.e. $> 1 \text{ g kg}^{-1}$) Ca-arsenates
56 and Ca-antimonates can control the As and Sb solubility (Johnson et al., 2005; Martínez-
57 Villegas et al., 2013). Furthermore, the highly insoluble tripuhyite ($FeSbO_4$) can control the Sb
58 solution concentration at very low levels ($\sim 1 \text{ ng L}^{-1}$), however the formation of this secondary
59 ferric antimonate mineral is likely slow, due to kinetic constraints (Leverett et al., 2012).
60 Finally, under moderately reducing conditions, poorly soluble Sb(III)–oxides like valentinite
61 and senarmonite (Sb_2O_3) could control the Sb solubility , while under sulphate–reducing
62 conditions, Sb(III)–sulfides (i.e. stibnite) can form (Bennett et al., 2017; Filella et al., 2009).

63 Lowering soil redox potential, e.g. due to waterlogging, is typically associated with
64 mobilisation of As, however exceptions and reverse trends have been documented (Frohne et
65 al., 2011; Hamon et al., 2004; Stroud et al., 2011; Williams et al., 2011). In contrast, anaerobic
66 conditions typically immobilise Sb and, again, some exceptions have been noted (Frohne et al.,
67 2011; Hockmann et al., 2014b, 2014a; Mitsunobu et al., 2006; Okkenhaug et al., 2012). The
68 mechanisms behind mobilization or immobilization of As and Sb upon reducing conditions are
69 rather complex, because changing redox conditions not only affects the speciation of As and
70 Sb, but also the properties of their sorbents which, in turn, influences strongly As and Sb
71 mobility. For example, reductive dissolution of Fe(III) and Mn (III, IV) hydroxides can release
72 previously bound As and Sb (Frohne et al., 2011; Hamon et al., 2004; Hockmann et al., 2014b;
73 Lovley, 1997). In contrast, Fe(II)-induced transformation of ferrihydrite to more crystalline
74 ferrihydrite and goethite under mild reducing conditions can immobilize Sb, likely by structural
75 incorporation of Sb(V) into the freshly formed Fe(III) hydroxide crystal lattice (Burton et al.,
76 2019).

77 Soil organic matter (SOM) can have a strong influence on redox-transformations of toxic
78 elements and of soil minerals (Borch et al., 2010), with different underlying mechanisms. First,
79 the presence of biodegradable carbon fuels i) aerobic respiration that will lead to anaerobic,
80 thus reducing conditions, when oxygen supply is limited and ii) anaerobic respiration that
81 enhances the reduction of redox-sensitive elements (Kulp et al., 2014; Oremland and Stolz,
82 2005). Next to this, humic substances play a role in redox cycling of As and Sb, or of their host
83 minerals Fe and Mn hydroxides by coupling the redox cycles of the redox-sensitive elements
84 to the redox cycles of quinone/hydroquinone functional groups present in the humic substances,
85 either directly or indirectly due to electron shuttling between electron donors and acceptors
86 (Jiang et al., 2009; Lovley et al., 1998; Qiao et al., 2019; Redman et al., 2002). Finally,
87 competition for sorption sites at Fe and Al hydroxide surfaces between humic substances and

88 As (Bauer and Blodau, 2006; Dousova et al., 2015; Gustafsson, 2006; Redman et al., 2002;
89 Verbeeck et al., 2017; Weng et al., 2009) or Sb (Karimian et al., 2019; Verbeeck et al., 2019),
90 may render As and Sb more available in soils for redox transformations. Thus, SOM could
91 influence redox-cycling of As and Sb and this can result in mobilisation or immobilisation of
92 As and Sb when soils get waterlogged. Furthermore, different underlying mechanisms can be
93 responsible for these changes in As and Sb retention, and this will likely depend on the local
94 composition of the organic matter, i.e. less or more biodegradable or less or more highly
95 reactive humic substances, similar as observed for aquifer sediments in the case of As (Guo et
96 al., 2019; Kulkarni et al., 2017). However, less information is available on this topic for Sb and
97 at background levels of both As and Sb in soils.

98 The objective of this study is to better understand the role of soil organic matter (SOM) on the
99 change in As and Sb mobility upon waterlogging soils. The hypothesis is that the presence of
100 SOM strongly affects the As and Sb mobility in waterlogged soils, and that the effects of SOM
101 on the change in As and Sb mobility combines different mechanisms i.e. being an electron
102 donor, electron shuttle or competitor for As and Sb species. To address this issue, the As and
103 Sb solid-liquid distribution was measured at low As and Sb concentrations in experimentally
104 waterlogged soils that i) have a natural gradient in SOM concentrations and ii) are amended
105 with or without glucose as an electron donor with neither electron shuttling nor competitive
106 effects on As and Sb sorption.

107 **2. Materials and methods**

108 *2.1. Soil samples and standard soil analysis*

109 A soil profile was excavated up to 3 m depth in a Stagnic Luvisol under agricultural grassland
110 in NE France (Crespy-le-Neuf, 48°24'11''N, 4°37'44''E). Nine samples were taken from
111 different depths, to obtain samples with a natural gradient in SOM concentration. The samples

112 were labelled P1_X with X the average sampling depth. All samples were sieved at 2 mm, air-
113 dried, and homogenized with a mortar and pestle prior to soil analysis.

114 Amorphous Fe, Al and manganese (Mn) and associated As were determined in a 0.2 M
115 ammonium oxalate extract at pH 3 (solid:liquid ratio 1:50, 2 hours equilibration in darkness;
116 Schwertmann (1964)) by inductively coupled plasma-mass spectrometry (ICP-MS, Agilent
117 7700x, Agilent Technologies, Santa Clara, CA, USA). Total Fe (hydr)oxide concentration was
118 determined by ICP-MS in a dithionite-citrate-bicarbonate (Fe_{DCB}) extract with an adapted
119 method based on Mehra and Jackson(1953). In short, 1 g air dry soil was weighed into a dark
120 50 ml centrifuge tube, 1 g of solid dithionite (Na₂S₂O₄; Fischer Scientific, Merelbeke, Belgium)
121 was added, followed by 50 ml of 0.3 M citrate – 0.1 M bicarbonate pH buffer. The samples
122 were warmed at 40°C in the oven for 3 h and then shaken (end-over-end) for 24 h at 19°C.
123 Finally, samples were centrifuged at 2500 g for 10 min and the supernatant was sufficiently
124 diluted before total Fe analysis with ICP-MS. The total organic carbon (OC) concentration of
125 the soil samples was determined by thermal oxidation at 900 °C, followed by gas
126 chromatographic measurements of the CO₂ generated (EA 1110, CE instruments, Wigan, UK)
127 after removal of carbonates with a 5% HCl solution. The dissolved organic carbon (DOC)
128 concentration was determined in a 1:10 solid:liquid ratio 5 mM Ca(NO₃)₂ soil extract as the
129 non-purgeable organic carbon (NPOC) by catalytic combustion and infrared detection of CO₂
130 (Multi NC-2100, AnalytikJena, Jena, Germany; Visco et al., 2005)). Soil pH was measured in
131 a 5 mM Ca(NO₃)₂ extract with a 1:10 solid:liquid ratio.

132 The total As concentration of the soil was determined by measuring the As concentration in an
133 *aqua regia* soil digest (3:1 ratio of concentrated HCl:HNO₃) with ICP-MS (helium gas was
134 used in the collision cell to remove interferences). Total soil Sb concentration was determined
135 by a four acid digestion, as described in Verbeeck et al. (2019) and here shortly repeated (full
136 protocol in the Supplementary data). Fifty mg of soil was weighed into Savillex beakers with

137 screw caps (Savillex, Eden Prairie, MN, USA). Concentrated HNO₃ (65%), HClO₄ (70%) and
138 HF (48%) were added consecutively, with digestion in a closed system and evaporation near
139 dry between each acid addition step and the residual digest was dissolved in 2.5 M HCl. The
140 Sb concentration in the digests was measured with ICP-MS at m/z = 121, without use of
141 reaction gas or collision cell. A reference sample (PACS-2 marine sediment, National Research
142 Council of Canada, Ottawa, Canada) with certified As and Sb concentrations was included
143 each batch in duplicate. All soil properties were analysed in duplicate, except for soil Sb that
144 was analysed without replicates.

145 *2.2. Arsenic and antimony sorption under different redox conditions*

146 The original samples that were collected moist in the field and stored at 4°C, were sieved at 4
147 mm. The field-moist soil samples had a gravimetric moisture content of on average 0.2 L kg⁻¹
148 oven-dry soil. The As and Sb sorption was determined by measuring the solid-liquid
149 distribution coefficient (K_D) on samples with four contrasting treatments: i) no treatment, initial
150 samples at moisture content as sampled; ii) aerobic incubation at moisture content as sampled
151 for 63 – 70 days; iii) anaerobic incubation under waterlogged conditions in an anaerobic
152 chamber (95% N₂, 5% H₂) for 63 – 70 days; iv) anaerobic incubations under waterlogged
153 conditions in an anaerobic chamber for 63 – 70 days, with the addition of glucose (5 g C per
154 kg soil; α-D-glucose, Sigma-Aldrich, Darmstadt, Germany) as electron donor and carbon
155 source to stimulate microbial respiration and subsequent reducing conditions. The relative long
156 incubation time was chosen to mimic seasonal periods of waterlogging. The different
157 treatments were made in duplicate.

158 *2.2.1. Arsenic sorption*

159 Arsenic K_D values were determined by single dose addition of the radio-tracer ⁷³As (as As(V),
160 Oak Ridge National Laboratory, Oak Ridge, TN, USA). This method enables the measurement

161 of the solid-liquid distribution of As without changing the soil equilibrium (Degryse et al.,
162 2009). For the initial samples, 2.5 g of field-moist soil was weighed out in a 50 ml centrifuge
163 tube with addition of 24 ml of a 5 mM CaCl₂ background solution and 1 ml of a carrier-free
164 ⁷³As stock (final activity of 5 – 26 kBq ml⁻¹, depending on estimated ⁷³As K_D values). Next,
165 the samples were placed in an end-over-end shaker for 7 days. For the aerobic incubation, about
166 30 g of field-moist soil was incubated at 19±2°C in closed 50 ml centrifuge tubes and after 63
167 days, 2.5 g of the incubated, field-moist soil was weighed out in a 50 ml centrifuge tube with
168 addition of 24 ml of a 5 mM CaCl₂ background solution and 1 ml of a carrier-free ⁷³As stock
169 (final activity of 5 – 26 kBq ml⁻¹, depending on estimated ⁷³As K_D values). Next, the samples
170 were placed in an end-over-end shaker for 7 days. For the anaerobic incubation, 5 g field-moist
171 soil was weighed into a 50 ml centrifuge tube, either or not with glucose addition, followed by
172 50 ml deoxygenated 5 mM CaCl₂. Glucose was added by weighing 63 mg of glucose in the
173 centrifuge tube before adding the soil (i.e. 5 g C kg⁻¹). The samples were shaken manually to
174 homogenize the soil, the solution and the added glucose. Then, for both anaerobic treatments,
175 the samples were pre-incubated in a water bath, completely submerged and at room
176 temperature, for one week before placing them in an anaerobic chamber (95% N₂, 5% H₂; on-
177 site constructed chamber) at room temperature. During the anaerobic incubation, the samples
178 were not further shaken. Resazurin solutions (1 mg L⁻¹; Acros Organics, Thermo Fischer
179 Scientific, Waltham, MA, USA) were used as an anaerobic indicator. Then, after 63 days of
180 anaerobic incubation, the previously incubated soil samples were opened in the anaerobic
181 chamber, 1 ml of the background solution was removed and replaced with 1 ml of ⁷³As spike
182 (final activity of 3 kBq ml⁻¹). Next, the samples were mounted on an end-over-end shaker in
183 the anaerobic chamber and shaken for 7 days.

184 After 7 days of end-over-end shaking, the soil suspensions of all treatments were left to
185 sediment, the supernatant was 0.45 µm filtered (Chromafil XtraPET -45/25) and the ⁷³As γ

186 activity (15–70 keV; Packard COBRA Auto-gamma A5003, GMI, Ramsey, MN, USA) was
187 measured. The K_D value for ^{73}As adsorption (in L kg^{-1}) was calculated as

$$188 \quad K_D \text{ } ^{73}\text{As} = \frac{(\gamma_i - \gamma_f) / W}{\gamma_f / V}, \quad (1)$$

189 where γ_i and γ_f are the total initial and final activity, respectively, of the added ^{73}As (Bq) in
190 solution, W is the mass of soil (oven-dry; kg) and V is the volume of the solution (L).

191 2.2.2. Antimony sorption

192 Antimony K_D values were measured by a single dose addition of 41 μmol of stable Sb(V) per
193 kg of soil. No radio-tracer was commercially available for Sb , however, the added Sb dose was
194 chosen to examine Sb sorption in the linear range, as suggested by sorption isotherms (Fan et
195 al., 2013; Martínez-Lladó et al., 2011; Verbeeck et al., 2019). In addition, the added Sb dose is
196 very comparable with the oxalate-extractable As concentration in the soils, i.e. the
197 concentration at which the solid-liquid distribution of both elements was evaluated is similar.
198 The incubation procedure, sampling and spiking method were also very similar to that used for
199 As . For the initial samples, 5 g soil (oven-dry basis) was weighed out in a 50 ml centrifuge tube
200 in two treatments, namely, 50 ml of 5 mM CaCl_2 was added, to obtain a non- Sb spiked, control
201 sample or 49.8 ml 5 mM CaCl_2 was added, followed by 0.2 ml of an Sb spike by a stock solution
202 (KSb(OH)_6 ; Sigma-Aldrich, Darmstadt, Germany), to obtain a Sb -spiked sample. Next,
203 samples were placed in an end-over-end shaker for 7 days. For the aerobic incubation, 5 g soil
204 (oven-dry basis) was incubated at $19 \pm 2^\circ\text{C}$ in closed 50 ml centrifuge tubes and after 56 days,
205 the same proceeding as for the initial samples was done, namely adding 50 ml of 5 mM CaCl_2
206 for control samples or adding 49.8 ml 5 mM CaCl_2 , followed by 0.2 ml of Sb spike by a stock
207 solution. Next, samples were placed in an end-over-end shaker for 7 days. For the anaerobic
208 incubation, 5 g soil (oven-dry basis) was weighed into a 50 ml centrifuge tube, either or not
209 with glucose addition, followed by addition of 50 ml deoxygenated 5 mM CaCl_2 . Glucose was

210 added and mixed with the soil suspension exactly as done for the As sorption assay, described
211 above. Then, for both anaerobic treatments, the samples were pre-incubated in a water bath,
212 completely submerged and at room temperature, for one week before placing them in an
213 anaerobic chamber (95% N₂, 5% H₂; Coy Lab's Vinyl Anaerobic Chambers (Coy Laboratory
214 Products Inc., Grass Lake, MI, USA)) at room temperature. During the anaerobic incubation,
215 the samples were not further shaken. Resazurin indicator strips (Oxoid Resazurin Anaerobic
216 Indicator, ThermoFischer Scientific, Waltham, MA, USA) were used as an anaerobic indicator.
217 Then, after 56 days of anaerobic incubation, the previously incubated soil samples were opened
218 in the anaerobic chamber, 0.2 ml of the background solution was removed and replaced with
219 0.2 ml of Sb spike, and also for this treatment, non-Sb spiked samples were included. Next, the
220 samples were mounted on an end-over-end shaker in the anaerobic chamber and shaken for 7
221 days.

222 After 7 days, the soil suspensions were allowed to settle, the supernatant was filtered over a
223 0.45 µm filter and the total Sb concentration in solution was measured by ICP-MS. The Sb K_D
224 values (in L kg⁻¹) were calculated as

$$225 \quad K_D \text{ Sb} = \frac{(M_{\text{sol},i} - (M_{\text{sol},f} - M_{\text{sol},c})) \times V/W}{M_{\text{sol},f} - M_{\text{sol},c}} \quad (2)$$

226 with M_{sol,i} and M_{sol,f} are the initial, resp. final concentrations of Sb in solution of the spiked
227 sample and M_{sol,c} is the concentration in solution of the naturally desorbing Sb, in a control,
228 non-Sb spiked soil sample (µM). The M_{sol,c} measurements are needed to correct the final
229 concentrations of the spiked samples, so only the fraction of added Sb that is adsorbed is
230 considered. Defined this way, the K_D values determine the sorption of added Sb, which, in case
231 of linear sorption, equals the solid-liquid distribution of the native, labile background Sb as
232 discussed elsewhere for the classification of K_D values (Degryse et al., 2009). Finally, W is the
233 weight of soil (oven-dry; kg) and V the volume of the solution (L).

234 2.3. *Solution composition*

235 In addition to the measurements of ^{73}As γ activity and Sb concentration, also DOC, total As,
236 Fe and Mn in solution (ICP-MS), As solution speciation and Fe solution speciation were
237 measured, with the latter two only in the anaerobic incubated samples.

238 The As speciation analysis was done by a microcartridge method with an anion exchanger resin
239 (Moreno-Jiménez et al., 2013). This speciation method is based on the hypothesis that the
240 neutral $\text{H}_3\text{AsO}_3^\circ$ will not be retained by the anion exchanger, while the negatively charged
241 $\text{H}_2\text{AsO}_4^-/\text{HAsO}_4^{2-}$ will be retained by the anion exchanger. The method is described in the
242 Supplementary data, and Table S1 presents the results of a preliminary test with model solution
243 of As(V)-As(III) mixtures. Only As speciation of the ^{75}As was measured, i.e. before and after
244 eluting the anaerobic supernatant over the anion exchange columns, the ^{75}As was measured by
245 ICP-MS, enabling us to measure the % of total soluble As that is present as As(III). The
246 speciation analysis was always performed within one day after sampling and inside the
247 anaerobic chamber. This method was also tested for Sb speciation analysis, but was found not
248 suitable for this (data not shown). No other method was used, thus no Sb speciation was
249 measured.

250 The Fe speciation analysis was done by the ferrozine method (Viollier et al., 2000), which
251 measures dissolved Fe(II). For this analysis, an acidified subsample of the supernatant was
252 used (0.1 M HNO_3). In acid conditions, Fe(II) oxidation is very slow (Davison and Seed, 1983),
253 ensuring Fe speciation preservation. The Fe(II) measurements were performed within one day
254 after sampling and outside of the anaerobic chamber.

255 Finally, the pH and redox potential (E_h) of the soil suspensions were measured with portable
256 field electrodes (WTW pH 91, Xylem Analytics, Weilheim, Germany and VWR ORP15,
257 Avantor, Central Valley, PA, USA), which are easy to use in the anaerobic chamber. This was

258 done after subsamples for the above described analyses were taken. The redox potential
259 measurement was controlled with saturated quinhydrone solutions at pH 4 and 7 (at 20°C or
260 25 °C; Alfa Aesar, Thermo Fischer Scientific, Waltham, MA, USA).

261 *2.4. Data analysis*

262 Statistical analyses were performed with the software package JMP Pro 13.1 from SAS
263 Institute Inc. (Cary, North Caroline, U.S.). The change in K_D values upon anaerobic incubation
264 was calculated as the ratio of the K_D value measured during anaerobic incubation with the mean
265 of the K_D value measured during the aerobic incubation of the corresponding soil sample.
266 Correlation analysis between measured soil and solution characteristics was done by
267 calculating the Pearson's correlation coefficient.

268 **3. Results**

269 *3.1. Soil properties*

270 The measured soil properties of the selected soil samples are presented in Table 1. The organic
271 carbon (OC) concentration ranged from below detection limit (1 g OC kg⁻¹ soil) to 39 g OC kg⁻¹
272 and the dissolved organic carbon (DOC) measured in a 1:10 solid:liquid 5 mM Ca(NO₃)₂ soil
273 extract ranged from below detection limit (0.5 mg DOC L⁻¹) to 18 mg DOC L⁻¹. The
274 concentration of amorphous Fe and Al in the samples of upper soil layers, up to about 1 m
275 depth, is higher than the concentration in samples from deeper soil layers. The total free Fe
276 oxides, determined with an dithionite–citrate–bicarbonate extraction, however is more constant
277 throughout the soil profile. This reflects in the amorphous Fe to total Fe oxide ratio
278 ($Fe_{ox}:Fe_{DCB}$), that is ~50 % in the uppermost soil layer to only 3% starting from about 1 m soil
279 depth. The detection limit for total soil As, determined by *aqua regia* digestion was 0.5 μmol
280 As kg⁻¹, well below the As concentrations in the tested soil samples, that ranged 91 – 223 μmol
281 As kg⁻¹. The detection limit of total soil Sb, determined by the four acid digestion, was 0.4

282 $\mu\text{mol Sb kg}^{-1}$, while the Sb concentrations of the tested soil samples ranged 3.4 – 4.9 $\mu\text{mol Sb}$
283 kg^{-1} . The PACS-2 reference sample has a certified As concentration of $350 \pm 20 \mu\text{mol As kg}^{-1}$
284 whereas $320 \pm 15 \mu\text{mol As kg}^{-1}$ was measured. The certified Sb concentration in the reference
285 sample was $93 \pm 21 \mu\text{mol Sb kg}^{-1}$ whereas $81 \pm 4 \mu\text{mol Sb kg}^{-1}$ was measured (means with
286 95% confidence interval). For all standard soil properties, the average coefficient of variation
287 (CV) of duplicate analysis was <9%, only for the DOC, this was 0.7 – 69%, on average 30%.

288 *3.2. As and Sb mobility under changing redox conditions*

289 Initially, the $^{73}\text{As } K_D$ values ranged 4000 – 140 000 L kg^{-1} between soil samples, while Sb K_D
290 values ranged 40 – 190 L kg^{-1} (Tables 2 and 3; full dataset presented in Table S2 and S3).
291 During the aerobic incubation, the K_D values of both elements did not change compared to the
292 initial samples. In contrast, large and contrasting changes in K_D values were noted upon
293 anaerobic incubation. The $^{73}\text{As } K_D$ values decreased by a factor of 80, on average, and even up
294 to a factor of 400 between aerobic and anaerobic incubated samples, with largest changes were
295 found in the SOM rich upper part of the sampled soil profile (Figure 1a). In contrast, Sb K_D
296 values increased by a factor of 5, on average, and up to a factor 20 after anaerobic incubation
297 compared to the aerobic incubation, with largest changes were again found in the SOM rich
298 upper soil layers (Figure 1b). The factor of change in K_D values upon anaerobic incubation, i.e.
299 $K_{D,AN} : K_{D,A}$, was significantly smaller for the subsoil samples, i.e. collected at more than 1 m
300 below surface, than for the surface soil samples, i.e. collected from the top 1 m, for both
301 elements (Figure 2). Glucose addition enhanced the changes in K_D values in the subsoil samples
302 for both elements whereas smaller and inconsistent effects were found in the topsoil samples
303 upon glucose addition, i.e. no additional changes in $^{73}\text{As } K_D$ values were noted while the
304 changes in Sb K_D were less pronounced than in the surface soils without glucose addition
305 (Figure 2). The factors change of $^{73}\text{As } K_D$ values and Sb K_D values are similar upon reducing
306 conditions when only soil organic matter (i.e. in surface soil) and when only glucose is present

307 (in glucose amended subsoil samples) (Figure 2), even when these factors change in K_D values
308 were normalized for the amount of OC present, i.e., the type of OC (i.e. only soil organic matter
309 or only glucose) did not influence the changes in As and Sb sorption upon anaerobic incubation
310 (Table 4).

311 Upon anaerobic incubation, the As concentrations in solution increased strongly, i.e. from
312 background concentrations of about 0.004 μM up to 1.5 μM soluble As, measured in the 1:10
313 solid:liquid 5 mM CaCl_2 soil extracts, and the As solution concentrations were strongly
314 negatively correlated with the measured ^{73}As K_D values ($r = -0.91$; $p < 0.0001$; based on \log_{10}
315 transformed data; data not shown), i.e. decreasing ^{73}As K_D values result in higher As mobility
316 in solution. During anaerobic incubation, the Sb concentrations in solution of the control, non-
317 Sb(V) spiked soil samples increased, from background concentrations of 0.2 nM to 10 nM
318 soluble Sb (Figure 3). This increase in solution Sb is matching the trend for As but contradicts
319 that of the Sb concentration in solution of the Sb(V) spiked soil, i.e. Sb concentrations in
320 solution of added Sb(V) decreased in reducing conditions, resulting in the increase in K_D
321 values, as shown in Figure 1b. The increase in natural Sb concentrations was largest in the
322 topsoil layers.

323 *3.3. Solution composition*

324 The As and Sb incubation tests ran at different times in different anaerobic chambers. In the
325 As adsorption assay, more negative E_h values and higher Fe(II) concentrations were noted
326 during anaerobic incubation than in the Sb adsorption assay, while Mn solution concentrations
327 were comparable (Tables 2 and 3; full dataset in Tables S2 and S3). In general, solution
328 properties remained constant in the aerobic incubated samples compared with the initial
329 samples. Soil pH changed during anaerobic conditions but trends were inconsistent, i.e.
330 increases and decreases were noted and the average absolute change in pH ($\Delta\text{pH} = |\text{pH}$

331 anaerobic – pH aerobic) was 0.4. Glucose addition acidified soils and the mean ΔpH
332 (compared to the aerobic soils) was 1.1, maximally 2. The As speciation data show that As(III)
333 concentrations ranged from below detection limit of the method (5 nM) to 1.2 μM . The %
334 As(III) of the total solution As ranged from non-detectable to 110% between samples, with no
335 clear effects of treatment (with or without glucose) or sampling location (subsoil or surface
336 soil) on As solution speciation (Table 2 and Figure S1).

337 *3.4. Correlations of As and Sb mobility with soil and solution properties under anaerobic* 338 *conditions*

339 The change in ^{73}As K_{D} upon anaerobic conditions ($K_{\text{D, AN}} : K_{\text{D, A}}$) was larger when Fe(II) and
340 Mn concentration in solution increased ($r = -0.82$; $p = 0.007$ for Fe(II) and $r = -0.95$; $p < 0.001$
341 for Mn respectively; correlation based on \log_{10} transformed data). These correlations were not
342 present in the anaerobic + glucose treatment. In the glucose amended samples however, the
343 change in ^{73}As K_{D} values was larger when the initial metal oxide concentration (quantified by
344 $\text{Fe}_{\text{DCB}} + \text{Mn}_{\text{ox}} + \text{Al}_{\text{ox}}$) was smaller ($r = -0.60$; $p = 0.009$; correlation based on \log_{10} transformed
345 K_{D} changes).

346 The changes in Sb K_{D} values in the anaerobic treatment increased significantly when the Mn
347 concentration in solution was higher and in samples with lower soil pH ($r = 0.93$, $p = 0.0008$
348 for Mn; $r = -0.93$, $p = 0.0008$ for pH; correlation based on \log_{10} transformed data except pH).
349 In the anaerobic + glucose treatment, only weak correlations were found (not shown). The
350 soluble Sb concentration in the control, non-Sb spiked samples, increased with increasing DOC
351 concentration in solution in the anaerobic treatment ($r = 0.87$, $p = 0.005$, correlation based on
352 \log_{10} transformed data; Figure 4).

353 Finally, in aerobic conditions, ^{73}As K_{D} values decreased with increasing OC concentrations
354 (Figure 5). Upon reducing conditions, ^{73}As K_{D} values decreased in topsoil samples, resulting

355 in a more steep decline of As sorption with increasing OC concentrations of the samples. In
356 addition, ^{73}As K_D values also decreased in glucose amended subsoil samples, but still, ^{73}As
357 sorption remains higher in low OC samples than in high OC samples (Figure 5). This was not
358 observed for Sb, only when Sb K_D values are normalized per molar concentrations of $\text{Fe}_{\text{ox}}+\text{Al}_{\text{ox}}$,
359 these K_D values do decrease with increasing OC in the aerobic treatment ($r = -0.61$; $p = 0.017$).

360 **4. Discussion**

361 This work was set up to identify the effects of soil organic matter on the changes in As and Sb
362 mobility upon reducing soils by flooding. The combination of a set of soils with i) a natural
363 SOM gradient and ii) the effects of either or no glucose additions, allows to disentangle the
364 different mechanisms by which SOM can mobilize or immobilize As and Sb under reducing
365 conditions.

366 When reducing conditions develop, As sorption decreases while Sb sorption increases
367 compared to aerobically incubated samples (Figure 1). This contrast between As and Sb was
368 observed in several previous studies (Arsic et al., 2018; Couture et al., 2015; Fu et al., 2016;
369 Mitsunobu et al., 2006). However, in our study, a striking difference in the extent of the changes
370 in As and Sb sorption was found between the uppermost layers (<1 m soil depth) and the deeper
371 soil layers (>1 m soil depth; Figure 2). This is most probably due to the lack of soil organic
372 matter in the deeper soil layers, which normally enhance redox processes in soils by i)
373 supporting aerobic respiration that induces reducing conditions in O_2 limited systems and ii)
374 mediating redox cycling of As, Sb and their host minerals, by supporting anaerobic respiration
375 or by enhancing these processes by electron shuttling. However, in our study, the different
376 types of organic carbon present (i.e. soil organic matter, glucose and combining both) did only
377 weakly affect the extent of change in As and Sb K_D values (Figure 2). In presence of only
378 glucose, i.e. in the glucose amended subsoil samples, the changes in As and Sb mobility are

379 comparable to the changes when only SOM is present, i.e. in the surface soil samples without
380 glucose amendment, even when these changes were corrected for the total amount of C present
381 (Table 4). This indicates that no additional effects of SOM, and more specifically of humic
382 substances, on the change in As and Sb sorption was observed compared to a mere carbon and
383 energy source for microbial metabolism, like glucose. This does not implicate that changes of
384 As and Sb sorption upon waterlogging cannot be facilitated by competitive or electron shuttling
385 effects of humic substances, as shown by several authors in the case of As (Jiang et al., 2009;
386 Qiao et al., 2019; Redman et al., 2002), but that the latter mechanisms likely contribute
387 relatively less to the overall change in As and Sb mobility under reducing conditions compared
388 to the carbon and electron donor effect of organic matter to stimulate microbial respiration.

389 The changes in ^{73}As K_D upon anaerobic incubation in presence of only native SOM, are most
390 likely due to the reductive dissolution of Fe(III) and Mn (III, IV) hydroxides and subsequent
391 loss of available sites for As sorption (Dixit and Hering, 2003; Villalobos et al., 2014). Different
392 studies point out the associations between Fe, Mn and As release to soil solution in reducing
393 conditions, due to the release of As by the reductive dissolution of Fe and Mn hydroxides
394 (Weber et al., 2010; Xu et al., 2017). Interestingly, the change in ^{73}As K_D was more strongly
395 correlated with dissolved Mn than with dissolved Fe(II) ($r = -0.82$; for Fe(II) and $r = -0.95$ for
396 Mn). This suggest that reductive dissolution of Mn hydroxides is more important for changes
397 in As mobility than dissolution of Fe hydroxides. However, As is usually more associated with
398 the Fe hydroxides than the Mn hydroxides in soils due i) to the higher affinity of As to Fe
399 oxides and ii) the usually higher abundance of Fe (hydr)oxides compared to Mn hydroxides
400 (Suda and Makino, 2016), what is indeed observed in our study (on average a factor of 8
401 higher). Possibly, the measured Fe(II) concentrations in solution are not reflecting directly the
402 reductive dissolution of Fe hydroxides due to complexation of the initially released Fe(II) with
403 the exchange complex in soil, while this could be less important for Mn(II). Indeed, Fe(II) can

404 be more strongly complexed by soil organic matter than Mn(II) (Dudal et al., 2005). In addition,
405 Fe(II) ions can be consumed during Mn(III, IV) hydroxide reductive dissolution (Postma and
406 Appelo, 2000). The results of our study do not indicate that redox transformation between
407 As(V) and As(III) resulted in the increased mobility of As in anaerobic condition, the As
408 speciation in solution did not explain the observed changes in ^{73}As K_D values upon reducing
409 conditions (Figure S1). This was also observed in a study by Hamon et al. (2004), i.e. the redox
410 speciation of As could be largely As(V) or As(III) in anaerobic conditions and
411 mobilisation/immobilisation of As under reducing conditions was a complex interplay between
412 changes in redox speciation, reductive dissolution of Fe hydroxides and pH changes during the
413 reducing conditions. When both sources of organic matter were present, i.e. SOM and glucose
414 in the surface soil sample, no enlarged effect on the changes in As K_D values was observed,
415 although more Fe(II) and Mn was released into solution than in the non-glucose amended
416 anaerobic treatment (Table 2). In these strongly reduced soils, the change in As K_D values was
417 likely not only controlled by mere dissolution of the metal hydroxides. Our data suggest that at
418 higher total hydroxide concentration in the initial, aerobic soil, the changes in ^{73}As K_D values
419 are lower ($r = -0.60$). When Fe and Mn hydroxides dissolve under reducing conditions,
420 As(V)/As(III) can still adsorb on the non-dissolved, more recalcitrant oxides, like the more
421 crystalline Fe oxides or the non-redox sensitive Al oxides, although likely to a lesser extent
422 than on the amorphous Fe hydroxides (Dixit and Hering, 2003; Goldberg, 2002). However, it
423 is difficult to estimate the amount of non-dissolved Fe oxides based only on the Fe(II) release,
424 due to the complexation of Fe(II) and use of Fe(II) as a reductant, as discussed above, but also
425 due to formation of Fe(II and/or III) minerals like siderite (FeCO_3) or like magnetite or
426 mackinawite in sulfate reducing conditions, which in turn also can provide additional sorption
427 sites for As (Burton et al., 2014, 2008; Tufano et al., 2008). Finally, this study corroborated the
428 general trend that increasing OC concentrations are associated with a decrease in As sorption

429 (Figure 5). When organic anions sorb to Fe and Al hydroxides, competition and electrostatic
430 repulsion result in lower As(V) in aerobic soils (Verbeeck et al., 2017). Interestingly, even
431 under strongly reducing conditions (+ glucose treatments), As sorption remains higher in the
432 low SOM containing soils (Figure 5), possibly indicating that the competition effects between
433 SOM and As species for sorption sites to the reactive minerals in the higher SOM containing
434 soils remain important in reducing conditions.

435 The changes in Sb K_D values upon anaerobic incubation in the presence of only native SOM
436 or only glucose may be partly related to reduction of the added Sb(V) to Sb(III). . The reduced
437 Sb(III) can be stronger retained to the residual, i.e. non-dissolved Fe(III) hydroxides at the pH
438 of the incubated soils (7 – 8), as observed by Leuz et al. (2006) on goethite at pH >7. The added
439 Sb(V) can be reduced biotically, by dissimilatory Sb(V) reducing bacteria (Kulp et al. (2014))
440 or abiotically, by interactions with freshly formed Fe(II) minerals in Fe(III) reducing conditions
441 (Kirsch et al., 2008; Mitsunobu et al., 2008) or by interactions with reduced humic substances,
442 when present (Karimian et al., 2019). Another mechanism that can explain increased Sb
443 retention in mildly reducing conditions is the incorporation of Sb(V) into the crystal lattice of
444 freshly formed Fe(III) hydroxides. Due to the similarities between Sb(V) and Fe(III) regarding
445 ion size (0.60 – 0.65 Å) and coordination number (6), Sb(V) can substitute for Fe(III) during
446 the Fe(II)-induced transformation of ferrihydrite into more crystalline Fe, which results in an
447 increased fixation of Sb (Burton et al., 2019; Mitsunobu et al., 2013). Unfortunately, no redox
448 or solid-phase speciation measurements of Sb are available to underpin these speculations.
449 Other mechanisms that could explain increased Sb retention are however unlikely to prevail,
450 i.e. during anaerobic incubation the pH of the samples only increased in some samples, which
451 would result in less Sb sorption (Leuz et al., 2006; Rakshit et al., 2011; Tighe et al., 2005),
452 which is contradictory to what was observed. When glucose was added during anaerobic
453 incubation, pH decreased in almost all samples, however, the change in pH could not solely

454 explain the change in sorption, with largest changes in K_D values not present in samples with
455 largest change in pH (Figure S2 in the Supporting Data). Next, it is very unlikely that increased
456 Sb sorption in our soils is due to precipitation of Sb(III) with oxides or sulphides, as the Sb
457 concentrations in solution of the spiked samples range 0.01 – 0.8 μM in both the anaerobic
458 treatments, which is lower than the equilibrium Sb concentration of $>1.8 \mu\text{M}$ of different
459 Sb(III) minerals at pH 7 and pH 5, calculated with the Visual Minteq 3.1 speciation program
460 (Gustafsson, 2019) for valentinite and senarmontite, both Sb(III) oxides and stibnite, an Sb(III)
461 sulphide. Finally, when glucose was added to the anaerobic incubated samples, changes in Sb
462 K_D values in surface soil layers are now smaller than in the subsoil layers ($<$ factor 10, Figure
463 1) and even in the uppermost soil layer of this experiment, the K_D values did not change
464 compared to the aerobic treatment. Also, in these samples, Fe(II) mobilisation is much larger
465 than in the anaerobically incubated samples without glucose addition (up to 2 700 μM Fe(II);
466 Table 3), so possibly loss of binding sites due to reductive dissolution of Fe hydroxides as a
467 consequence of anaerobic respiration, counteracts the increased Sb(III) retention. These results
468 are similar to what Hockmann et al. (2014b) observed, i.e. increased Sb retention under
469 moderately reducing conditions, due to reduction of Sb(V) to Sb(III), followed by release of
470 Sb in Fe-reducing conditions.

471 Finally, the changes in the geogenic Sb solution concentration upon anaerobic incubation were
472 contradictory to the changes of the Sb K_D values, i.e. solution Sb concentration increased, while
473 Sb K_D values decreased (Figure 1 and 3). Possibly, this can be explained by reduction of Sb(V)
474 to Sb(III) and subsequent complexation of Sb(III) with DOC. The reduced Sb(III) is more
475 strongly complexed with DOC than Sb(V) at pH values above 4 (Tella and Pokrovski, 2012,
476 2009) and this could explain the observed mobilisation of Sb in the control samples (up to
477 factor of 10; Figure 3) upon anaerobic conditions, together with a small increase in DOC
478 concentrations upon anaerobic incubation (up to a factor of 3; Table S3). This mechanisms is

479 likely not playing an important role in the changes of Sb mobility in the Sb spiked samples,
480 due to the overall low complexation capacity of DOC for Sb(III), although higher than for
481 Sb(V), in combination with low DOC concentrations (i.e., maximum 12 mg DOC L⁻¹) in the
482 samples from this study. In the non Sb-spiked samples, the Sb:DOC ratio in solution of the
483 surface samples (<60 cm soil depth) increased from ~ 0.3 nmol Sb per mg DOC to ~ 0.8 nmol
484 Sb per mg DOC, upon anaerobic incubation. This Sb:DOC ratio is similar as reported by
485 Buschmann and Sigg (2004), i.e. ~ 0.7 nmol Sb per mg DOC, at similar DOC and total Sb
486 concentration (i.e. 5 mg DOC l⁻¹ and 8 nM Sb). However, the total Sb concentration in the Sb-
487 spiked samples is much higher, i.e. ~ 0.4 μM, resulting in a Sb:DOC ratio of ~100 nmol Sb per
488 mg DOC in the aerobic incubated surface samples. Buschmann and Sigg (2004) report a
489 maximum complexing capacity of 4 – 60 nmol Sb per mg DOC for Aldrich humic acid and
490 Suwannee River humic acid, which is lower than observed in the samples of this study, which
491 makes mobilisation of Sb with DOC at higher Sb concentrations likely not feasible. The
492 complexation of Sb(III) to the reactive functional groups of soil organic matter could however
493 be more important in soils with higher organic matter concentrations than in the soils used in
494 this study, and the higher Sb(III) than Sb(V) complexation can result in an increased retention
495 of Sb when reducing conditions arise (Besold et al., 2019).

496 **5. Conclusions**

497 Soil organic matter strongly alters the mobility of As and Sb in anaerobic soils. Changes of the
498 As and Sb mobility under reducing conditions are significantly higher and thus more important
499 towards As and Sb migration in the SOM rich surface soils compared to smaller changes in
500 samples collected at >1 m below surface. In general, the extent of *change* in As and Sb mobility
501 due to the presence of SOM in anaerobic conditions, can be largely explained by its effects as
502 electron donor during microbial respiration. In addition, at low Sb concentrations, the
503 complexation capacity of dissolved organic matter could increase Sb mobility. Finally, the

504 *absolute* K_D value of As under waterlogged conditions remains affected by SOM as a
505 competitive ligand, i.e. lower mobility in low SOM containing soil, suggesting that SOM still
506 acts as competitive ligand for As sorption even in strongly reduced conditions.

507 **Acknowledgements**

508 We thank the Agence national pour la gestion des déchets radioactifs (Andra) for funding this
509 study, Joeri Plevoets for his help in the lab and Kristin Coorevits and Elvira Vassilieva for their
510 help with the four acid digestion.

511 **References**

- 512 Arsic, M., Teasdale, P.R., Welsh, D.T., Johnston, S.G., Burton, E.D., Hockmann, K.,
513 Bennett, W.W., 2018. Diffusive gradients in thin films (DGT) reveals antimony and
514 arsenic mobility differs in a contaminated wetland sediment during an oxic-anoxic
515 transition. *Environ. Sci. Technol.* 52, 1118–1127.
516 <https://doi.org/10.1021/acs.est.7b03882>
- 517 Bauer, M., Blodau, C., 2006. Mobilization of arsenic by dissolved organic matter from iron
518 oxides, soils and sediments. *Sci. Total Environ.* 354, 179–190.
519 <https://doi.org/10.1016/j.scitotenv.2005.01.027>
- 520 Bennett, W.W., Hockmann, K., Johnston, S.G., Burton, E.D., 2017. Synchrotron X-ray
521 absorption spectroscopy reveals antimony sequestration by reduced sulfur in a
522 freshwater wetland sediment. *Environ. Chem.* 14, 345–349.
523 <https://doi.org/10.1071/en16198>
- 524 Besold, J., Kumar, N., Scheinost, A.C., Pacheco, J.L., Fendorf, S., Planer-Friedrich, B., 2019.
525 Antimonite Complexation with Thiol and Carboxyl/Phenol Groups of Peat Organic
526 Matter. *Environ. Sci. Technol.* 53, 5005–5015. <https://doi.org/10.1021/acs.est.9b00495>
- 527 Borch, T., Kretzschmar, R., Kappler, A., Van Cappellen, P., Ginder-Vogel, M., Voegelin, A.,
528 Campbell, K., 2010. Biogeochemical Redox Processes and their Impact on Contaminant
529 Dynamics. *Environ. Sci. Technol.* 44, 15–23. <https://doi.org/10.1021/es9026248>
- 530 Burton, E.D., Bush, R.T., Sullivan, L.A., Johnston, S.G., Hocking, R.K., 2008. Mobility of
531 arsenic and selected metals during re- flooding of iron- and organic-rich acid-sulfate
532 soil. *Chem. Geol.* 253, 64–73. <https://doi.org/10.1016/j.chemgeo.2008.04.006>
- 533 Burton, E.D., Hockmann, K., Karimian, N., Johnston, S.G., 2019. Antimony mobility in

534 reducing environments: The effect of microbial iron(III)-reduction and associated
535 secondary mineralization. *Geochim. Cosmochim. Acta* 245, 278–289.
536 <https://doi.org/10.1016/j.gca.2018.11.005>

537 Burton, E.D., Johnston, S.G., Kocar, B.D., 2014. Arsenic Mobility during Flooding of
538 Contaminated Soil: The Effect of Microbial Sulfate Reduction. *Environ. Sci. Technol.*
539 48, 13660–13667. <https://doi.org/10.1021/es503963k>

540 Buschmann, J., Sigg, L., 2004. Antimony(III) binding to humic substances: Influence of pH
541 and type of humic acid. *Environ. Sci. Technol.* 38, 4535–4541.
542 <https://doi.org/10.1021/es049901o>

543 Couture, R.M., Charlet, L., Markelova, E., Madé, B., Parsons, C.T., 2015. On-off
544 mobilization of contaminants in soils during redox oscillations. *Environ. Sci. Technol.*
545 49, 3015–3023. <https://doi.org/10.1021/es5061879>

546 Davison, W., Seed, G., 1983. The kinetics of the oxidation of ferrous iron in synthetic and
547 natural waters. *Geochim. Cosmochim. Acta* 47, 67–79. [https://doi.org/10.1016/0016-](https://doi.org/10.1016/0016-7037(83)90091-1)
548 [7037\(83\)90091-1](https://doi.org/10.1016/0016-7037(83)90091-1)

549 Degryse, F., Smolders, E., Parker, D.R., 2009. Partitioning of metals (Cd, Co, Cu, Ni, Pb, Zn)
550 in soils: concepts, methodologies, prediction and applications - a review. *Eur. J. Soil Sci.*
551 60, 590–612. <https://doi.org/10.1111/j.1365-2389.2009.01142.x>

552 Dixit, S., Hering, J.G., 2003. Comparison of arsenic(V) and arsenic(III) sorption onto iron
553 oxide minerals: Implications for arsenic mobility. *Environ. Sci. Technol.* 37, 4182–4189.
554 <https://doi.org/10.1021/es030309t>

555 Dousova, B., Buzek, F., Herzogova, L., Machovic, V., Lhotka, M., 2015. Effect of organic
556 matter on arsenic(V) and antimony(V) adsorption in soils. *Eur. J. Soil Sci.* 66, 74–82.

557 <https://doi.org/10.1111/ejss.12206>

558 Dudal, Y., Se, G., Dupont, L., Guillon, E., 2005. Fate of the metal-binding soluble organic
559 matter throughout a soil profile. *Soil Sci.* 170, 707–715.
560 <https://doi.org/10.1097/01.ss.0000185909.03213.6b>

561 Fan, J.X., Wang, Y.J., Cui, X.D., Zhou, D.M., 2013. Sorption isotherms and kinetics of
562 Sb(V) on several Chinese soils with different physicochemical properties. *J. Soils
563 Sediments* 13, 344–353. <https://doi.org/10.1007/s11368-012-0612-z>

564 Filella, M., May, P., 2003. Computer simulation of the low-molecular-weight inorganic
565 species distribution of antimony (III) and antimony (V) in natural waters. *Geochim.
566 Cosmochim. Acta* 67, 4013–4031. [https://doi.org/10.1016/S0016-7037\(03\)00095-4](https://doi.org/10.1016/S0016-7037(03)00095-4)

567 Filella, M., Williams, P.A., Belzile, N., 2009. Antimony in the environment: Knowns and
568 unknowns. *Environ. Chem.* 6, 95–105. <https://doi.org/10.1071/EN09007>

569 Frohne, T., Rinklebe, J., Diaz-Bone, R.A., Du Laing, G., 2011. Controlled variation of redox
570 conditions in a floodplain soil: Impact on metal mobilization and biomethylation of
571 arsenic and antimony. *Geoderma* 160, 414–424.
572 <https://doi.org/10.1016/j.geoderma.2010.10.012>

573 Fu, Z., Zhang, G., Li, H., Chen, J., Liu, F., Wu, Q., 2016. Influence of reducing conditions on
574 the release of antimony and arsenic from a tailings sediment. *J. Soils Sediments* 16,
575 2471–2481. <https://doi.org/10.1007/s11368-016-1484-4>

576 Goldberg, S., 2002. Competitive Adsorption of Arsenate and Arsenite on Oxides and Clay
577 Minerals. *Soil Sci. Soc. Am. J.* 66, 413–421. <https://doi.org/10.2136/sssaj2002.4130>

578 Guo, H., Li, X., Xiu, W., He, W., Cao, Y., Zhang, D., Wang, A., 2019. Controls of organic
579 matter bioreactivity on arsenic mobility in shallow aquifers of the Hetao Basin, P.R.

580 China. *J. Hydrol.* 571, 448–459. <https://doi.org/10.1016/j.jhydrol.2019.01.076>

581 Gustafsson, J.P., 2019. Visual MINTEQ version 3.1. Available online at
582 <https://vminteq.lwr.kth.se/>.

583 Gustafsson, J.P., 2006. Arsenate adsorption to soils: Modelling the competition from humic
584 substances. *Geoderma* 136, 320–330. <https://doi.org/10.1016/j.geoderma.2006.03.046>

585 Hamon, R.E., Lombi, E., Fortunati, P., Nolan, A.L., McLaughlin, M.J., 2004. Coupling
586 Speciation and Isotope Dilution Techniques to Study Arsenic Mobilization in the
587 Environment. *Environ. Sci. Technol.* 38, 1794–1798. <https://doi.org/10.1021/es034931x>

588 Hockmann, K., Lenz, M., Tandy, S., Nachtegaal, M., Janousch, M., Schulin, R., 2014a.
589 Release of antimony from contaminated soil induced by redox changes. *J. Hazard.
590 Mater.* 275, 215–221. <https://doi.org/10.1016/j.jhazmat.2014.04.065>

591 Hockmann, K., Tandy, S., Lenz, M., Schulin, R., 2014b. Antimony leaching from
592 contaminated soil under manganese- and iron-reducing conditions: column experiments.
593 *Environ. Chem.* 11, 624–631. <https://doi.org/10.1071/en14123>

594 Jiang, J., Bauer, I., Paul, A., Kappler, A., 2009. Arsenic redox changes by microbially and
595 chemically formed semiquinone radicals and hydroquinones in a humic substance model
596 quinone. *Environ. Sci. Technol.* 43, 3639–3645. <https://doi.org/10.1021/es803112a>

597 Johnson, C.A., Moench, H., Wersin, P., Kugler, P., Wenger, C., 2005. Solubility of antimony
598 and other elements in samples taken from shooting ranges. *J. Environ. Qual.* 34, 248–54.
599 <https://doi.org/10.2134/jeq2005.0248>

600 Karimian, N., Burton, E.D., Johnston, S.G., Hockmann, K., Choppala, G., 2019. Humic acid
601 impacts antimony partitioning and speciation during iron (II) -induced ferrihydrite
602 transformation. *Sci. Total Environ.* 683, 399–410.

603 <https://doi.org/10.1016/j.scitotenv.2019.05.305>

604 Kirsch, R., Scheinost, A.C., Rossberg, A., Banerjee, D., Charlet, L., 2008. Reduction of
605 antimony by nano-particulate magnetite and mackinawite. *Mineral. Mag.* 72, 185–189.
606 <https://doi.org/10.1180/minmag.2008.072.1.185>

607 Kulkarni, H. V., Mladenov, N., Johannesson, K.H., Datta, S., 2017. Contrasting dissolved
608 organic matter quality in groundwater in Holocene and Pleistocene aquifers and
609 implications for influencing arsenic mobility. *Appl. Geochemistry* 77, 194–205.
610 <https://doi.org/10.1016/j.apgeochem.2016.06.002>

611 Kulp, T.R., Miller, L.G., Braiotta, F., Webb, S.M., Kocar, B.D., Blum, J.S., Oremland, R.S.,
612 2014. Microbiological reduction of Sb(V) in anoxic freshwater sediments. *Environ. Sci.*
613 *Technol.* 48, 218–226. <https://doi.org/10.1021/es403312j>

614 Leuz, A., Mönch, H., Johnson, C.A., 2006. Sorption of Sb (III) and Sb (V) to goethite :
615 influence on Sb (III) oxidation and mobilization. *Environ. Sci. Technol.* 40, 7277–7282.
616 <https://doi.org/10.1021/es061284b>

617 Leverett, P., Reynolds, J.K., Roper, A.J., Williams, P.A., 2012. Tripuhyite and schafarzikite :
618 two of the ultimate sinks for antimony in the natural environment. *Mineral. Mag.* 76,
619 891–902. <https://doi.org/10.1180/minmag.2012.076.4.06>

620 Lovley, D., 1997. Microbial Fe (III) reduction in subsurface environments. *FEMS Microbiol.*
621 *Rev.* 20, 305–313. <https://doi.org/10.1111/j.1574-6976.1997.tb00316.x>

622 Lovley, D.R., Fraga, J.L., Blunt-Harris, E.L., Hayes, L.A., Phillips, E.J.P., Coates, J.D., 1998.
623 Humic substances as a mediator for microbially catalyzed metal reduction. *Acta*
624 *Hydrochim. Hydrobiol.* 26, 152–157. [https://doi.org/10.1002/\(SICI\)1521-](https://doi.org/10.1002/(SICI)1521-401X(199805)26:3<152::AID-AHEH152>3.0.CO;2-D)
625 [401X\(199805\)26:3<152::AID-AHEH152>3.0.CO;2-D](https://doi.org/10.1002/(SICI)1521-401X(199805)26:3<152::AID-AHEH152>3.0.CO;2-D)

- 626 Mandal, B.K., Suzuki, K.T., 2002. Arsenic round the world: a review. *Talanta* 58, 201–235.
627 [https://doi.org/10.1016/S0039-9140\(02\)00268-0](https://doi.org/10.1016/S0039-9140(02)00268-0)
- 628 Martínez-Lladó, X., Valderrama, C., Rovira, M., Martí, V., Giménez, J., de Pablo, J., 2011.
629 Sorption and mobility of Sb(V) in calcareous soils of Catalonia (NE Spain): Batch and
630 column experiments. *Geoderma* 160, 468–476.
631 <https://doi.org/10.1016/j.geoderma.2010.10.017>
- 632 Martínez-Villegas, N., Briones-Gallardo, R., Ramos-Leal, J.A., Avalos-Borja, M., Castañón-
633 Sandoval, A.D., Razo-Flores, E., Villalobos, M., 2013. Arsenic mobility controlled by
634 solid calcium arsenates: A case study in Mexico showcasing a potentially widespread
635 environmental problem. *Environ. Pollut.* 176, 114–122.
636 <https://doi.org/10.1016/j.envpol.2012.12.025>
- 637 Masscheleyn, P.H., Delaune, R.D., Patrick, W.H., 1991. Effect of redox potential and pH on
638 arsenic speciation and solubility in a contaminated soil. *Environ. Sci. Technol.* 25,
639 1414–1419. <https://doi.org/https://doi.org/10.1021/es00020a008>
- 640 Mehra, O.P., Jackson, M.L., 1953. Iron oxide removal from soils and clays by a dithionite-
641 citrate system buffered with sodium bicarbonate. *Clays Clay Miner.* 7, 317–327.
- 642 Mitsunobu, S., Harada, T., Takahashi, Y., 2006. Comparison of antimony behavior with that
643 of arsenic under various soil redox conditions. *Environ. Sci. Technol.* 40, 7270–7276.
644 <https://doi.org/https://doi.org/10.1021/es060694x>
- 645 Mitsunobu, S., Muramatsu, C., Watanabe, K., Sakata, M., 2013. Behavior of antimony(V)
646 during the transformation of ferrihydrite and its environmental implications. *Environ.*
647 *Sci. Technol.* 47, 9660–9667. <https://doi.org/10.1021/es4010398>
- 648 Mitsunobu, S., Takahashi, Y., Sakai, Y., 2008. Abiotic reduction of antimony(V) by green

649 rust ($\text{Fe}_4(\text{II})\text{Fe}_2(\text{III})(\text{OH})_{12}\text{SO}_4 \cdot 3\text{H}_2\text{O}$). *Chemosphere* 70, 942–947.
650 <https://doi.org/10.1016/j.chemosphere.2007.07.021>

651 Mitsunobu, S., Takahashi, Y., Terada, Y., 2010. μ -XANES Evidence for the Reduction of
652 Sb(V) to Sb(III) in Soil from Sb Mine Tailing. *Environ. Sci. Technol.* 44, 1281–1287.
653 <https://doi.org/10.1021/es902942z>

654 Moreno-Jiménez, E., Six, L., Williams, P.N., Smolders, E., 2013. Inorganic species of arsenic
655 in soil solution determined by microcartridges and ferrihydrite-based diffusive gradient
656 in thin films (DGT). *Talanta* 104, 83–89. <https://doi.org/10.1016/j.talanta.2012.11.007>

657 Okkenhaug, G., Zhu, Y.G., He, J., Li, X., Luo, L., Mulder, J., 2012. Antimony (Sb) and
658 Arsenic (As) in Sb mining impacted paddy soil from Xikuangshan, China: Differences
659 in mechanisms controlling soil sequestration and uptake in Rice. *Environ. Sci. Technol.*
660 46, 3155–3162. <https://doi.org/10.1021/es2022472>

661 Oremland, R.S., Stolz, J.F., 2005. Arsenic, microbes and contaminated aquifers. *Trends*
662 *Microbiol.* 13, 45–49. <https://doi.org/10.1126/science.1102374>

663 Postma, D., Appelo, C.A.J., 2000. Reduction of Mn-oxides by ferrous iron in a flow system:
664 Column experiment and reactive transport modeling. *Geochim. Cosmochim. Acta* 64,
665 1237–1247. [https://doi.org/doi.org/10.1016/S0016-7037\(99\)00356-7](https://doi.org/doi.org/10.1016/S0016-7037(99)00356-7)

666 Qiao, J., Li, X., Li, F., Liu, T., Young, L.Y., Huang, W., Sun, K., Tong, H., Hu, M., 2019.
667 Humic Substances Facilitate Arsenic Reduction and Release in Flooded Paddy Soil.
668 *Environ. Sci. Technol.* 53, 5034–5042. <https://doi.org/10.1021/acs.est.8b06333>

669 Rakshit, S., Sarkar, D., Punamiya, P., Datta, R., 2011. Antimony sorption at gibbsite-water
670 interface. *Chemosphere* 84, 480–483.
671 <https://doi.org/10.1016/j.chemosphere.2011.03.028>

672 Redman, A.D., Macalady, D.L., Ahmann, D., 2002. Natural organic matter affects arsenic
673 speciation and sorption onto hematite. *Environ. Sci. Technol.* 36, 2889–2896.
674 <https://doi.org/10.1021/es0112801>

675 Schwertmann, U., 1964. Differenzierung der Eisenoxide des Bodens durch Extraktion mit
676 Ammoniumoxalat-Lösung (The differentiation of iron oxides in soils by extraction
677 with ammonium oxalate solution). *Zeitschrift für Pflanzenernährung, Düngung,*
678 *Bodenkd.* 105, 194–202.

679 Stroud, J.L., Khan, M.A., Norton, G.J., Islam, M.R., Dasgupta, T., Zhu, Y.G., Price, A.H.,
680 Meharg, A.A., McGrath, S.P., Zhao, F.J., 2011. Assessing the labile arsenic pool in
681 contaminated paddy soils by isotopic dilution techniques and simple extractions.
682 *Environ. Sci. Technol.* 45, 4262–4269. <https://doi.org/10.1021/es104080s>

683 Suda, A., Makino, T., 2016. Functional effects of manganese and iron oxides on the
684 dynamics of trace elements in soils with a special focus on arsenic and cadmium: A
685 review. *Geoderma* 270, 68–75. <https://doi.org/10.1016/j.geoderma.2015.12.017>

686 Tella, M., Pokrovski, G.S., 2012. Stability and structure of pentavalent antimony complexes
687 with aqueous organic ligands. *Chem. Geol.* 292–293, 57–68.
688 <https://doi.org/10.1016/j.chemgeo.2011.11.004>

689 Tella, M., Pokrovski, G.S., 2009. Antimony(III) complexing with O-bearing organic ligands
690 in aqueous solution: An X-ray absorption fine structure spectroscopy and solubility
691 study. *Geochim. Cosmochim. Acta* 73, 268–290.
692 <https://doi.org/10.1016/j.gca.2008.10.014>

693 Tighe, M., Lockwood, P., Wilson, S., 2005. Adsorption of antimony(v) by floodplain soils,
694 amorphous iron(III) hydroxide and humic acid. *J. Environ. Monit.* 7, 1177–1185.
695 <https://doi.org/10.1039/b508302h>

696 Tufano, K.J., Reyes, C., Saltikov, C.W., Fendorf, S., 2008. Reductive Processes Control
697 Arsenic Retention: Revealing Relative Importance of Iron and Arsenic Reduction.
698 Environ. Sci. Technol. 42, 1–10. [https://doi.org/https://doi.org/10.1021/es801059s](https://doi.org/10.1021/es801059s)

699 Verbeeck, M., Hiemstra, T., Thiry, Y., Smolders, E., 2017. Soil organic matter reduces the
700 sorption of arsenate and phosphate: a soil profile study and geochemical modelling. Eur.
701 J. Soil Sci. 68, 678–688. <https://doi.org/10.1111/ejss.12447>

702 Verbeeck, M., Warrinnier, R., Gustafsson, J.P., Thiry, Y., Smolders, E., 2019. Soil organic
703 matter increases antimonate mobility in soil: An Sb(OH)₆ sorption and modelling study.
704 Appl. Geochemistry 104, 33–41. <https://doi.org/10.1016/j.apgeochem.2019.03.012>

705 Villalobos, M., Escobar-Quiroz, I.N., Salazar-Camacho, C., 2014. The influence of particle
706 size and structure on the sorption and oxidation behavior of birnessite: I. Adsorption of
707 As(V) and oxidation of As(III). Geochim. Cosmochim. Acta 125, 564–581.
708 <https://doi.org/10.1016/j.gca.2013.10.029>

709 Viollier, E., Inglett, P.W., Hunter, K., Roychoudhury, A.N., Van Cappellen, P., 2000. The
710 Ferrozine method revisited: Fe(II)/Fe(III) determination in natural waters. Appl.
711 Geochemistry 15, 785–790. [https://doi.org/10.1016/S0883-2927\(99\)00097-9](https://doi.org/10.1016/S0883-2927(99)00097-9)

712 Visco, G., Campanella, L., Nobili, V., 2005. Organic carbons and TOC in waters : an
713 overview of the international norm for its measurements. Microchem. J. 79, 185–191.
714 <https://doi.org/10.1016/j.microc.2004.10.018>

715 Weber, F.A., Hofacker, A.F., Voegelin, A., Kretzschmar, R., 2010. Temperature dependence
716 and coupling of iron and arsenic reduction and release during flooding of a contaminated
717 soil. Environ. Sci. Technol. 44, 116–122. <https://doi.org/10.1021/es902100h>

718 Weng, L., Van Riemsdijk, W.H., Hiemstra, T., 2009. Effects of fulvic and humic acids on

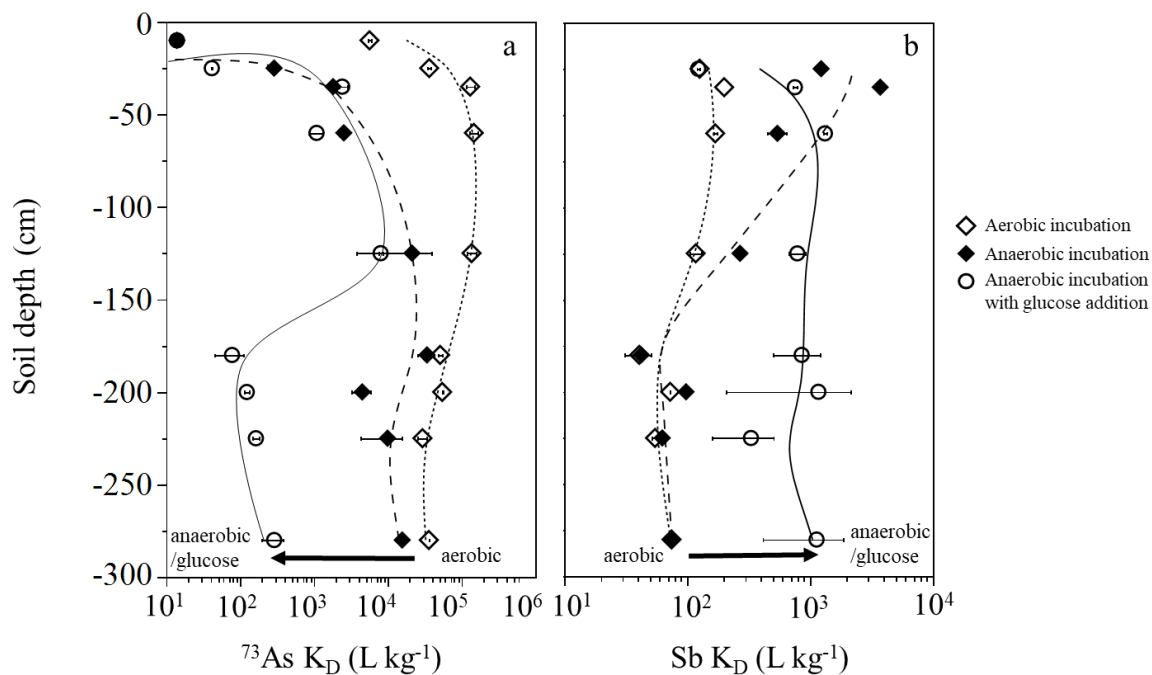
719 arsenate adsorption to goethite: Experiments and modeling. *Environ. Sci. Technol.* 43,
720 7198–7204. <https://doi.org/10.1021/es9000196>

721 Williams, P.N., Zhang, H., Davison, W., Meharg, A.A., Hossain, M., Norton, G.J., Brammer,
722 H., Islam, M.R., 2011. Organic matter-solid phase interactions are critical for predicting
723 arsenic release and plant uptake in Bangladesh paddy soils. *Environ. Sci. Technol.* 45,
724 6080–6087. <https://doi.org/10.1021/es2003765>

725 Wilson, S.C., Lockwood, P. V., Ashley, P.M., Tighe, M., 2010. The chemistry and behaviour
726 of antimony in the soil environment with comparisons to arsenic: A critical review.
727 *Environ. Pollut.* 158, 1169–1181. <https://doi.org/10.1016/j.envpol.2009.10.045>

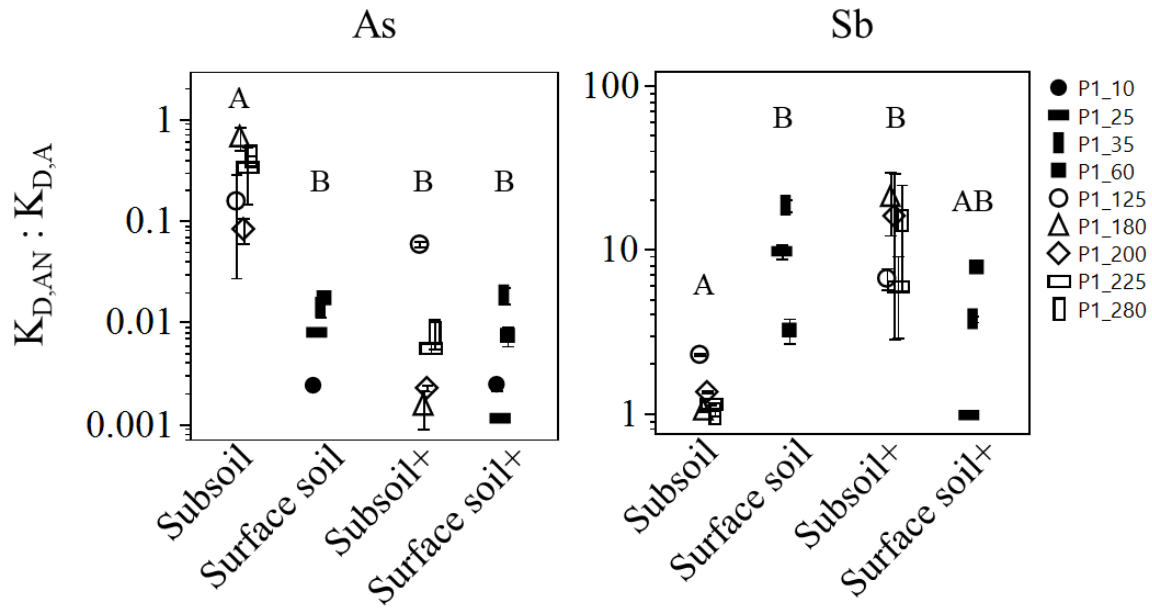
728 Xu, X., Chen, C., Wang, P., Kretzschmar, R., Zhao, F.-J., 2017. Control of arsenic
729 mobilization in paddy soils by manganese and iron oxides. *Environ. Pollut.* 231, 37–47.
730 <https://doi.org/10.1016/j.envpol.2017.07.084>

731



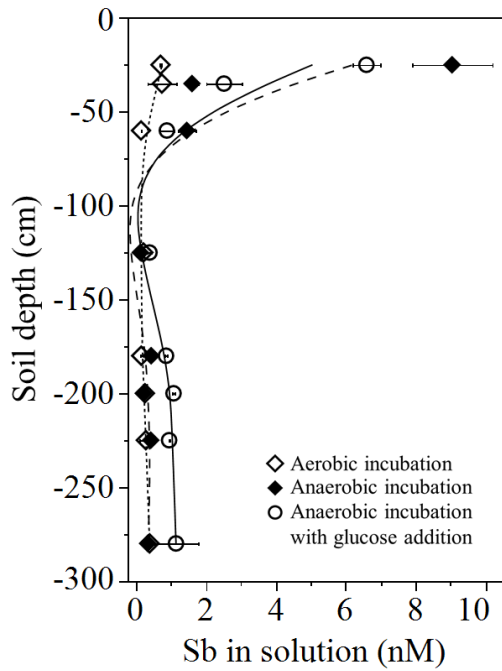
733

734 **Fig. 1.** When aerobic conditions change into anaerobic conditions (arrow), $^{73}\text{As } K_D$ values
 735 decrease (a) while $\text{Sb } K_D$ values increase (b) and these changes in K_D are more pronounced in
 736 topsoil layers (0–60 cm below surface) than in the bottom of the soil profile. Upon glucose
 737 addition during anaerobic conditions, further decrease (As) or increase (Sb) of K_D values are
 738 more pronounced in the subsoil layers (>160 cm soil depth) than in the topsoil. Mean values
 739 with error bars presenting one standard error are presented ($n=2$). Lines are added to guide the
 740 eye.



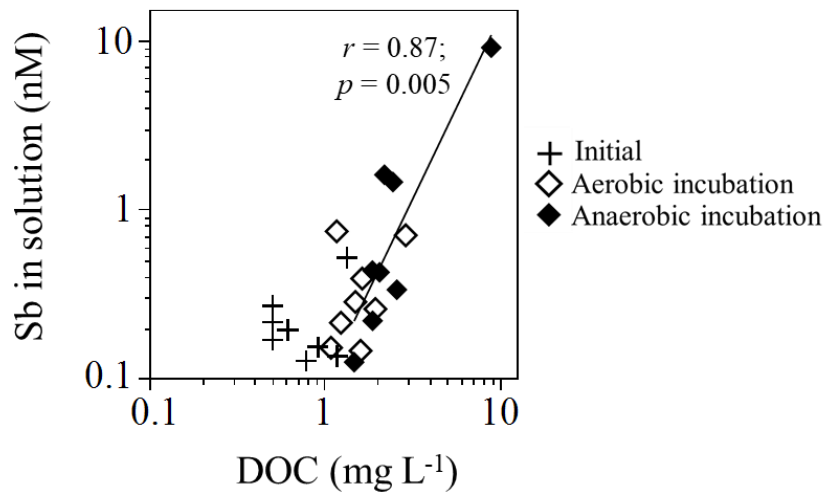
741

742 **Fig. 2.** Factor of change in ^{73}As K_D (left graph) and Sb K_D (right graph) between anaerobically
 743 and aerobically incubated surface soil and subsoil samples, with 1 m below surface the
 744 threshold between surface and subsoil. Samples were either or not amended with glucose (+),
 745 enabling to compare samples with very low OC (Subsoil), only with soil organic matter (SOM)
 746 (Surface), only with glucose present (Subsoil+) and with both types of OC present, i.e. SOM
 747 & glucose (Surface+). Mean data of replicate analyses are presented with error bars presenting
 748 one standard error ($n=2$). Letters connect groups with means which are not significantly
 749 different ($\alpha=0.05$; Tukey HSD test on \log_{10} transformed data).



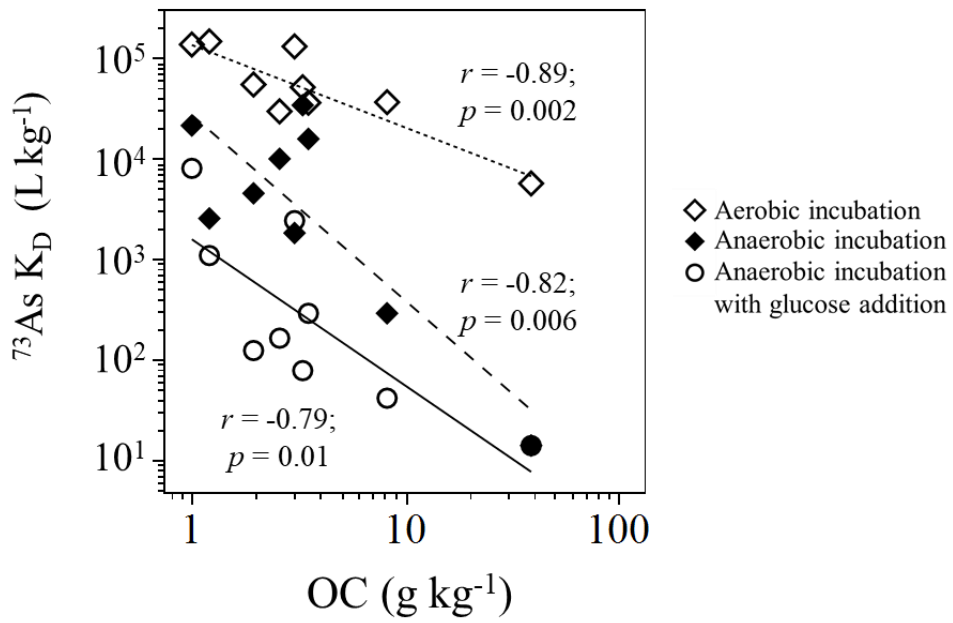
750

751 **Fig. 3.** Sb in solution in control, non-Sb spiked samples increases in topsoil layers when
 752 reducing conditions develop. Mean values with error bars presenting one standard error are
 753 presented ($n=2$). Lines are to guide the eye.



754

755 **Fig. 4.** The Sb concentration in solution increased with increasing DOC concentration in the
 756 anaerobic incubated samples (without glucose addition), suggesting mobilization of Sb by
 757 DOC. Mean datais presented ($n=2$). The regression line is presented to guide the eye.



758

759 **Fig. 5.** $^{73}\text{As } K_D$ values decrease with increasing organic carbon content, in all treatments. Mean
 760 data are presented ($n=2$). Lines are regressions and presented to guide the eye.

761 **Tables**762 **Table 1**

763 Soil properties of collected soil samples ($n=9$). Mean values from duplicate analyses are presented, except for total Sb, which was determined
764 without replicates.

Sample	pH	OC ^a (g kg ⁻¹)	DOC ^b (mg L ⁻¹)	Fe _{ox} ^c	Fe _{DCB} ^d (mmol kg ⁻¹)	Al _{ox} ^c	Mn _{ox} ^c	Fe _{ox} : Fe _{DCB}	As _{ar} ^e	As _{ox} ^c (μmol kg ⁻¹)	Sb _{tot} ^f
P1_10	5.5	39	18	83	169	23	5.3	0.49	91	53	3.4
P1_25	6.6	8	3.7	47	258	25	7.0	0.18	111	47	4.5
P1_35	6.6	3	1.0	20	244	30	4.3	0.08	123	29	3.9
P1_60	7.1	1	0.8	11	269	34	1.5	0.04	117	29	4.4
P1_125	7.1	<1	<0.5	11	290	24	14	0.04	189	39	4.9
P1_180	6.9	3	<0.5	6	180	10	1.0	0.03	151	26	3.8
P1_200	7.6	2	<0.5	8	264	14	2.4	0.03	148	23	4.5
P1_225	7.0	3	<0.5	7	275	15	0.6	0.03	181	24	3.7
P1_280	7.5	4	<0.5	7	254	12	0.5	0.03	223	25	3.6

765 ^aorganic carbon; ^bdissolved organic carbon; ^coxalate extractable; ^ddithionite-citrate-bicarbonate extractable; ^e*aqua regia* extractable As; ^fSb
766 extracted with four acid digestion

767 **Table 2**

768 Properties of the 5 mM CaCl₂ extracts of soils before and after 70 days (an)aerobic incubation in the As adsorption/desorption assay. Median
 769 (minimum-maximum) of nine different samples of a soil profile are presented (*n*=9).

Treatment	⁷³ As K _D (L kg ⁻¹)	As in solution (μM)	As mobilized as As(III) (%)	Eh vs SHE (mV)	pH	DOC (mg L ⁻¹)	Fe(II) in solution ————— (μM)	Mn in solution ————— (μM)
Initial	49 000 (4 000 – 140 000)	0.004 (<0.002 – 0.007)	n.a.	370 (200 – 410)	7.5 (6.1 – 7.7)	n.a.	n.a.	0.013 (<0.005 – 0.69)
Aerobic	50 000 (5 200 – 160 000)	0.004 (<0.002 – 0.027)	n.a.	150 (140 – 360)	7.7 (6.1 – 7.9)	n.a.	n.a.	0.011 (<0.005 – 0.35)
Anaerobic	3 300 (12 – 42 000)	0.011 (<0.002 – 1.5)	72 (n.d. – 96)	63 (-15 – 400)	7.0 (6.4 – 7.9)	n.a.	1.3 (<1 – 970)	8 (0.5 – 150)
Anaerobic + glucose	160 (12 – 7 900)	0.27 (0.047 – 1.5)	57 (2 – 110)	77 (-8 – 290)	6.7 (5.4 – 7.2)	320 (75 – 380)	1800 (57 – 5000)	120 (3 – 930)

770 n.a. = not available; n.d. = not detectable

771

772 **Table 3**

773 Properties of the 5 mM CaCl₂ extracts of soils before and after 63 days (an)aerobic incubation in the Sb adsorption/desorption assay. Median
 774 (minimum-maximum) of eight different sample of a soil profile are presented (*n*=8).

Treatment	Sb K _D (L kg ⁻¹)	Sb in solution	Sb in solution	Eh vs SHE (mV)	pH	DOC (mg L ⁻¹)	Fe(II) in solution	Mn in solution (μM)
		in control samples	in spiked samples					
Initial	95 (37 – 200)	0.18 (0.08 – 0.58)	386 (186 – 857)	n.a.	7.1 (6.4 – 7.5)	1 (<0.5 – 2)	n.a.	0.006 (<0.005 – 0.12)
Aerobic	77 (30 – 200)	0.30 (0.10 – 1.6)	498 (204 – 1032)	300 (240 – 340)	7.7 (6.4 – 8.0)	2 (1 – 3)	n.a.	0.01 (<0.005 – 0.4)
Anaerobic	180 (42 – 4 100)	0.44 (0.12 – 10)	276 (12 – 812)	190 (100 – 360)	7.7 (7.0 – 8.0)	2 (1 – 12)	<1 (<1 – 7)	4 (0.5 – 200)
Anaerobic + glucose	700 (120 – 2 100)	1.0 (0.33 – 7.0)	63 (21 – 335)	180 (85 – 290)	6.4 (5.4 – 6.8)	340 (310 – 380)	1100 (51 – 2700)	100 (8 – 680)

775 n.a. = not available

776 **Table 4** The factor of change in ⁷³As and Sb K_D values for subsoil samples (collected at >1 m
 777 soil depth), surface samples (collected at <1 m soil depth) and subsoil and surface samples
 778 amended with glucose (Subsoil/Surface+), normalized by the amount of C present in the soil
 779 sample during the anaerobic incubation (measured OC + added glucose-C when applicable).

	K _{D, AN} : K _{D, A} (g ⁻¹ OC)	
	As	Sb
Subsoil	0.13 ^A	0.8 ^A
Surface soil	0.005 ^B	3.3 ^A
Subsoil +	0.002 ^B	1.7 ^A
Surface soil +	0.001 ^B	0.6 ^A

780 Mean values of soil samples per group (subsoil or surface soil) are presented and connected
 781 with the same letter when not significantly different from each other ($\alpha=0.05$; Tukey HSD
 782 test on log₁₀ transformed data).